mater.scichina.com link.springer.com

Published online 1 April 2024 | https://doi.org/10.1007/s40843-023-2794-7
Sci China Mater 2024, 67(5): 1491–1499

Intrinsically healing conducting polymer/hydrogel nanocomposite films and their novel volumetric channel for high-performance, flexible, and healable organic phototransistors

Yujie Yan[1,2†*], Xiaoting Zhu[3†], Guocheng Zhang[4], Xiumei Wang[5], Xiao Han[1], Weizhou Li[1], Dongya Sun[1], Yuechan Li[1], Yi Wang[1], An Xie[1*] and Huipeng Chen[2*]

ABSTRACT **The flexible organic phototransistors (OPTs) are crucial for next-generation wearable systems for applications where large mechanical deformation is involved. However, most of the reported OPTs utilizing the field-effect transistor (FET) architecture suffer from undesired mechanical flexibility and limited performance due to their interfacial charge transport and inherently low transconductance; moreover, their π-conjugated semiconductor polymers that serve as channels lack specific healing sites, making it difficult to intrinsically heal themselves. Herein, a more flexible and high-performance OPT with enhanced interfacial charge transport *via* novel volumetric channel and strong healing capability is developed for the first time. This OPT utilizes an organic electrochemical transistor architecture that consists of intrinsically healing conducting polymer/hydrogel composite films with three-dimensional volumetric channels. Such devices not only efficiently restore their mechanical and electrical performance in 100 ms after undergoing severe damage but also exhibit excellent mechanical flexibility without obviously degraded performance. More importantly, the self-healing OPTs exhibit high performance with a responsivity as high as 1.01×10^5 A W^{-1}, detectivity of 1.75×10^{12} Jones, and high external quantum efficiency of 3.03×10^4%, higher than those of the majority of the reported FET-based OPTs. All of these results indicate that these novel and intrinsically self-healing OPTs with volumetric channels are ideal for use in next-generation wearable devices.**

Keywords: electrochemical transistor, interface, phototransistor, healing, volumetric channel, flexibility

INTRODUCTION

To meet the increasing demands for next-generation wearable optoelectronic devices and systems, an ideal flexible organic phototransistor (OPT) is required to have good stretchability, flexibility, and high photoresponse when undergoing repeated mechanical bending operations [1–4]. OPTs have been widely utilized in many industrial and military fields, including biomedical sensors, optical communication, and night vision [5–10]. Considerable efforts have been currently devoted to improving the mechanical flexibility and softness of organic materials for developing highly flexible OPTs [3,11–16]. However, the intrinsic characteristics of the device (including the interface, working mechanism, and transconductance) that are also crucial factors for determining the mechanical flexibility and electronic performance of the entire device have rarely received attention.

To date, most of the reported OPTs have been based on the field-effect transistor (FET) architecture [17–19], where their charges are accumulated and transported within the first few monolayers of the semiconductor film at the dielectric/semiconductor interface [19]. This feature makes charge transport susceptible to the cracks inside the channel that were formed when undergoing repeated mechanical bending, largely deteriorating their flexibility and, thus, optoelectronic performance. Improving the charge transport at the dielectric/semiconductor interface is important for achieving high-performance OPTs. Meanwhile, FET-based OPTs suffer from limited transconductance values of several microsiemens because their charge transport only occurs at the dielectric/semiconductor interface, which results in low device capacitance [20]. Transconductance is an important parameter that directly determines the capability of OPTs to amplify the incident light and its change after illuminating [21]. Therefore, the performance improvement of OPTs based on FETs is significantly impeded by their two-dimensional (2D) charge transport property. Compared with that in FETs, charge accumulation and transportation in organic electrochemical transistors (OECTs) occurs over the entire volumetric channel (3D channel), leading to their larger device capacitance and thus ultrahigh transconductance [22,23]. In this respect, OECTs have higher transconductance values by a few

[1] School of Materials Science and Engineering, Xiamen University of Technology, Key Laboratory of Functional Materials and Applications of Fujian Province, Xiamen Key Laboratory of High Performance Metals and Materials, Xiamen University, Xiamen 361024, China
[2] Institute of Optoelectronic Display, National & Local United Engineering Laboratory of Flat Panel Display Technology, Fuzhou University, Fuzhou 350002, China
[3] Joint School of National University of Singapore and Tianjin University, International Campus of Tianjin University, Fuzhou 350207, China
[4] Fujian University of Technology, Fuzhou 350108, China
[5] School of Engineering, Anhui Agricultural University, Hefei 230036, China
† These authors contributed equally to this work.
* Corresponding authors (emails: hpchen@fzu.edu.cn (Chen H); yujieyan@t.xmut.edu.cn (Yan Y); anxie@xmut.edu.cn (Xie A))

© Science China Press 2024

millisiemens than organic electrolyte-gated transistors [24–26], through which biological sensors and electrophysiological recorders based on OECTs achieve higher sensitivity than those based on FETs because of their higher inherent amplification function that enables them to amplify small signals [27–30]. However, the use of OECT device systems with high transconductance values and novel volumetric channels to construct OPTs has rarely been investigated, which is particularly promising for improving their optoelectronic performance and flexibility.

Self-healing is a crucial feature in natural biological systems, through which organs and tissues can spontaneously repair themselves after undergoing damage [31,32]. Therefore, another alternative to further improve the mechanical flexibility of OPTs is rendering them with self-healing capability that enables them to recover damaged areas instead of preventing them. Self-healing electronic devices based on self-healing materials can recover both mechanical and electronic performance from severe damage by reforming the reversible hydrogen bond, ionic interaction, and metal–ligand interactions [1,33–35], thereby significantly enhancing the robustness, flexibility, and durability of these devices and extending their working life [35]. However, OPTs capable of intrinsically self-healing themselves without adding healing agents under mechanical damage have yet to be realized because their π-conjugated semiconductor polymers lack specific bonding sites, including ionic bonding, reversible covalent bonding, and hydrogen bonding (mainly with relatively weak van der Waals interaction, <10 kcal mol^{-1}) [36].

In this study, we develop an intrinsically healing and biodegradable phototransistor with a novel volumetric channel based on CdSe/ZnS-poly(3,4-ethylenedioxythiophene):poly(styrenesulfonate) (PEDOT:PSS)/hydrogel composite coatings to further improve the flexibility and optoelectronic performance of OPTs. PEDOT:PSS and ionic hydrogel films exhibit strong healing capability upon mechanical damage *via* the reformation of the dynamic hydrogen bonds and electrostatic force. Notably, the CdSe/ZnS-PEDOT:PSS/hydrogel composite films can also be dissolved in water, exhibiting their biodegradability. OPTs fabricated from these materials can be repaired and thus restore their optoelectronic performance after cutting and healing. Furthermore, the self-healing OPTs exhibit high performance in terms of a responsivity as high as 1.01×10^5 A W^{-1}, detectivity of 1.75×10^{12} Jones, and high external quantum efficiency (EQE) of 3.03×10^4%. This study opens up the possibility of the application of OECTs in self-healing, highly sensitive, and flexible photodetectors.

EXPERIMENTAL SECTION

Material preparation and characterization

The ionic hydrogel was first prepared by dissolving 333 mg (lithium bis(trifluoromethane)sulfonamide (LiTFSI); >99%; Sigma-Aldrich) and 1.34 g carboxylated chitosan (Aladdin) in 5 mL deionized (DI) water. Then, the solution was stirred at 50°C for 5 h to form a clear, homogeneous, and viscous gel. The CdSe/ZnS-PEDOT:PSS solution was prepared by mixing cadmium selenide/zinc sulfide-alloyed quantum dots (CdSe/ZnS QDs; 5 mg mL^{-1}; Suzhou Xingshuo Mesolight Co., Ltd.) with PEDOT:PSS (Clevios PH1000, Heraeus Holding GmbH) at a weight ratio of 3:7. The morphological characterization of the CdSe/ZnS-PEDOT:PSS blend solution was conducted *via* transmission electron microscopy (TEM, Tecnai G2F20). The optical morphology images were acquired by a fluorescence microscope (BX51M, Olympus). The thickness of the films was determined using the Alpha-Step D-600. The optical absorption spectra measurements were recorded by the Cary 300 ultraviolet–visible spectrometer (UV–vis; Agilent Technologies). The Physical Electronics Model 5400 electron spectrometer (Thermo Scientific ESCALAB 250) was used to record the ultraviolet photoelectron spectra (UPS).

Self-healing conditions and tests

For the self-healing tests, the films were cut using a razor blade, with the cut widths ranging between 1 and 50 μm. Then, the damaged films were healed by dropping approximately 5 μL of DI water to cover the damaged area. Consequently, the healed films were placed on a 60°C hot plate for 60 s to remove DI water. Finally, the morphology and optoelectronic performance of the healed films and OPTs were further characterized and tested.

Device fabrication and analysis

The polyethylene (PET) with indium tin oxide (ITO) substrates were cleaned through an ultrasonic bath in acetone, isopropanol, and DI water for 15 min and dried using nitrogen gas. Afterward, the PET with ITO substrates were blade-coated with ionic hydrogel at a blade gap and velocity of 300 μm and 15 mm s^{-1}, respectively. Then, the deposited film was annealed in an oven at 50°C for 24 h. Subsequently, the CdSe/ZnS-PEDOT:PSS film was prepared by spin-coating with a spin rate of 2000 r min^{-1} in the hydrogel film and annealed at 120°C for 1 h. Finally, the Au source and drain electrodes (the thickness of 50 nm) were fabricated by thermal evaporation through a shadow mask with a channel length of 30 μm and a channel width of 1000 μm. The electrical performance of the device was measured by the Keithley 4200A SCS parameter analyzer in air. The monochromatic light with adjustable power intensity was derived from a 300-W wavelength-adjustable xenon lamp source (Beijing NBET Technology Co., Ltd., Omno302).

RESULTS AND DISCUSSION

Device architecture and its functional layer chemical structures

Fig. 1a shows the 3D device architecture diagram of the intrinsically healing and flexible OPTs. Their detailed fabrication process is presented in the EXPERIMENTAL SECTION. The active layer consists of the CdSe/ZnS QDs and PEDOT:PSS hybrid where the water-soluble CdSe/ZnS QDs are regarded as the photo-absorbing materials and PEDOT:PSS serves as a carrier transport channel. The optimized weight ratio of PEDOT:PSS and CdSe/ZnS is set as 7:3 because this hybrid not only ensures sufficient light absorption but also efficiently provides a charge transport channel and healing volumetric component, ensuring that a high optoelectronic and self-healing performance is achieved in self-healing OPTs. To characterize the morphology of the CdSe/ZnS-PEDOT:PSS hybrid, high-resolution TEM was conducted, as shown in Fig. 1b. The CdSe/ZnS QDs are uniformly dispersed in the PEDOT:PSS matrix, which is also confirmed by the obvious elemental peaks of Cd, Se, Zn, and S detected from CdSe/ZnS-PEDOT:PSS hybrid film (Fig. 1c). To realize a self-healing electrolyte layer, hydrogels consisting of chitosan and LiTFSI are selected because of their healing

 © Science China Press 2024

characteristics resulting from reversible hydrogen bonding. Their chemical structures are illustrated in Fig. 1d, e.

Healing property of conducting polymer/hydrogel composite films

To examine the healing capacity of the CdSe/ZnS-PEDOT:PSS channel and hydrogel in OPTs, the fresh CdSe/ZnS-PEDOT:PSS/hydrogel composite films were completely cut by a razor blade, as shown in Fig. 2e. A cut interface with a gap of approximately 40 μm was detected, and its area was larger than the thickness of the composite film (approximately 700 nm, as shown in Fig. S1) and comparable to the channel area of the self-healing OPTs, which is an obstacle to realizing an efficient self-healing process. Subsequently, the gap in the composite films

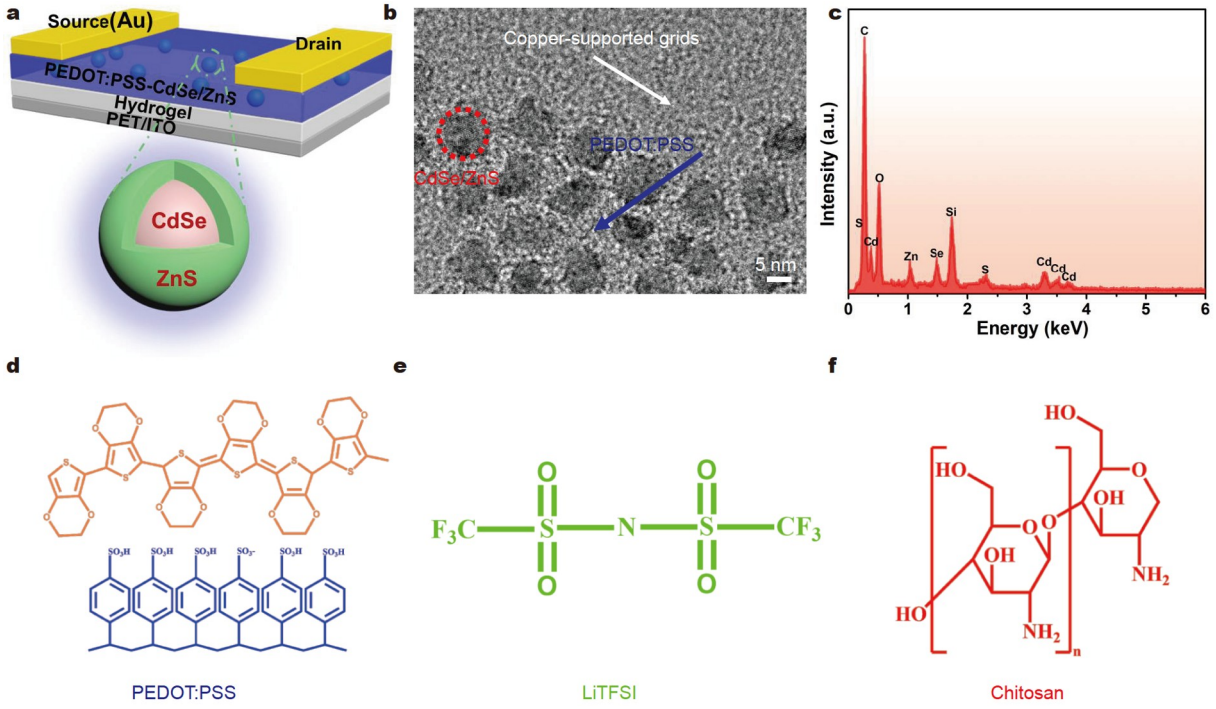

Figure 1 (a) Device architecture of the healing OPTs based on CdSe/ZnS-PEDOT:PSS/hydrogel/ITO/PET (top) and schematic of CdSe/ZnS QDs (bottom). (b) High-resolution TEM image of the CdSe/ZnS-PEDOT:PSS hybrid. (c) Energy dispersive X-ray spectroscopy elemental spot of the CdSe/ZnS-PEDOT:PSS layer. (d–f) Chemical structures of PEDOT:PSS and hydrogel.

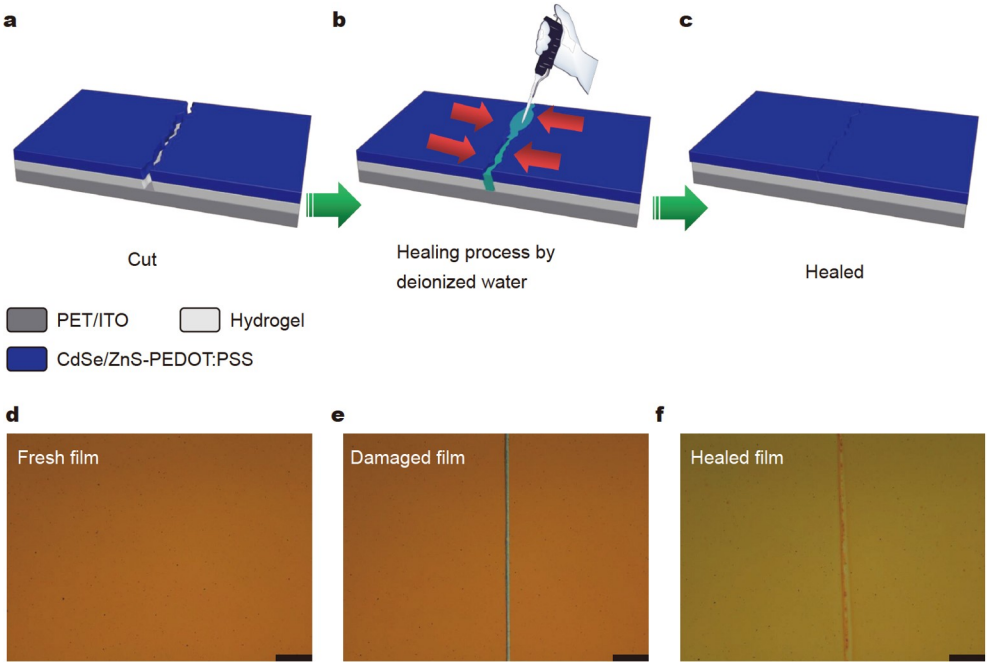

Figure 2 (a–c) Schematic of the water-induced healing process in the CdSe/ZnS-PEDO:PSS/hydrogel composite films and (d–f) the corresponding optical images. Scale bar: 200 μm.

© Science China Press 2024

was largely healed by dropping approximately 5 μL of DI water to cover the damaged area, as shown in Fig. 2b, f, confirming the efficient healing process of the CdSe/ZnS-PEDOT:PSS/hydrogel composite films by water. Moreover, the healing processes of hydrogel-only and CdSe/ZnS-PEDOT:PSS-only films were observed, as shown in Figs S2 and S3, respectively, indicating their healing capabilities.

To obtain insights into the healing process of the composite film, dynamic electrical breakdown healing experiments were performed at a constant voltage of 1 V, followed by cutting the film with a razor blade and healing with DI water, as shown in Fig. 3a. When the CdSe/ZnS-PEDOT:PSS/hydrogel composite films were severely damaged, the conductivity of the films sharply declined from the original value of 10^{-3} to 10^{-9} A under ambient conditions. Once the cut interface was in contact with DI water, the conductivity of the films immediately recovered to 10^{-4} A with a rapid healing time of approximately 100 ms (Fig. 3b), which indicated that the damaged films had been successfully healed by DI water. To further verify the reliability and reproducibility of the water-induced healing process, the cutting/healing experiments at different locations were repeated six times, as shown in Fig. S4. Notably, the current was stabilized when conducting the first cutting/healing cycle, indicating that the CdSe/ZnS-PEDOT:PSS/hydrogel composite films have efficient and reliable healing capability. Moreover, the conductivity of the composite films slightly decreased after healing, which was attributed to the slight destruction of the composite films by DI water during the healing process because of their water-soluble property. However, the CdSe/ZnS-PEDOT:PSS/hydrogel composite films show relatively good reliability and reproducibility because of the small amount of DI water (approximately 5 μL) needed to repair the composite films and the subsequent annealing to remove DI water, which minimizes the destruction of the composite films by DI water. Furthermore, the CdSe/ZnS-PEDOT:PSS/hydrogel composite films were easily biodegraded when the amount of DI water was continually increased to 500 μL to overwhelm the entire film, as shown in Fig. S5. Biodegradability is also an important biomimetic capability of next-generation wearable optoelectronic devices and systems, and it can significantly reduce the increment in electronic waste [37].

Healing properties and flexibility of phototransistors based on composite films

The intrinsically healing and flexible OPTs based on CdSe/ZnS-PEDOT:PSS/hydrogel composite films were fabricated and investigated, as shown in Fig. 4, in which the devices consisted of an organic channel (CdSe/ZnS-PEDOT:PSS) that was in direct contact with a solid electrolyte (chitosan:LiTFSI) and PET/ITO that served as a flexible substrate and the gate electrode. The self-healing OPTs were configured with a channel length L of 30 μm and a width W of 1000 μm. When the device channel was scratched using a razor blade, the damaged area could be observed in Fig. 4a. The representative transfer property characterizing transistor performance is illustrated in Fig. 4e, in which the channel current (I_{DS}) of the damaged OPTs cannot be regulated by the gate voltage, and its value only reached a current of 10^{-9} A, indicating that the channel suffered from severe cracking. By contrast, the healed OPTs exhibited a depletion-type representative controlled gate transistor property, which is the same as the initial device before cutting, as shown in Fig. 4d, indicating the efficient healing of the damaged channel and hydrogel film (Fig. 4c). Meanwhile, a high transconductance value of 4 mS was achieved, which is important for realizing high-responsivity OPTs. All of these results indicate that the OPTs using healable CdSe/ZnS-PEDOT:PSS/hydrogel composite films have an efficient healing capability. Furthermore, the mechanical properties of the flexible OPTs were investigated. Fig. S6 shows the photograph of OPTs under a bending state. The flexible devices showed similar electrical performance in terms of the transfer and transconductance characteristics before and after bending with a bending radius of 18 mm, as shown in Fig. S7a. To obtain more insights, when the bending time was increased to 500 times with a bending radius of 18 mm, the peak transconductance and on-state current of the device still retained high values of 3.0 mS and 0.85 mA, respectively, which are over 85% of their original values (Fig. S7b). These results indicate that the self-healing OPTs have strong endurance and mechanical robustness, which are attributed to both the inherently flexible PEDOT:PSS/hydrogel composite films and the volumetric charge transport property of the device that makes charges less affected by the interfaces and cracks inside the channel during mechanical bending (Fig. S13d).

Photoelectric performance of healing phototransistors

The photoelectric characteristics of the self-healing OPTs are further measured and investigated after cutting and healing. Fig. 5a shows the absorption spectra of the CdSe/ZnS QDs film in the UV–vis range, and the QDs exhibit strong UV light

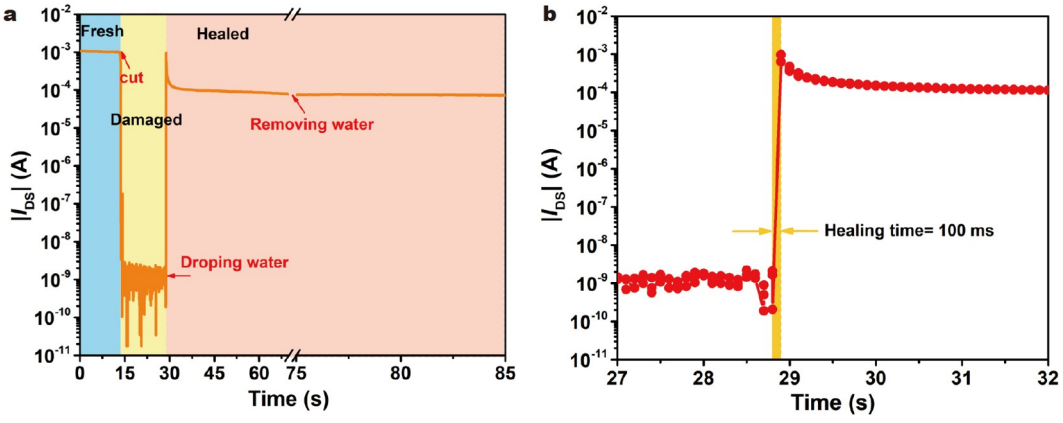

Figure 3 (a) Dynamic electrical measurements of the CdSe/ZnS-PEDOT:PSS/hydrogel composite films during the entire healing process. (b) Time-dependent transient current response of the composite films when uptaking water.

© Science China Press 2024

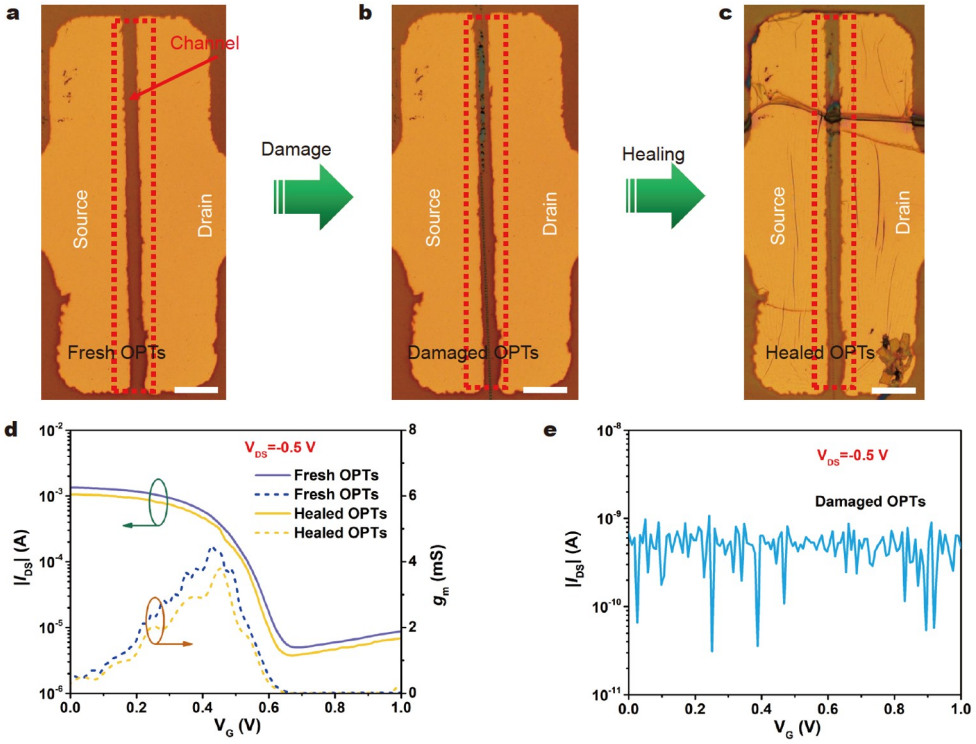

Figure 4 (a–c) Optical images of the healing and flexible OPTs based on the CdSe/ZnS-PEDO:PSS/hydrogel composite films before cutting and after healing on the channel. Scale bar: 100 μm. (d, e) Transfer and transconductance curves of the fresh, damaged, and healed devices.

absorption. Fig. 5b shows the schematic of the healed OPTs working under 365-nm illumination. The device transfer property was achieved under different UV light (365 nm) intensities ranging from 5 to 1000 μW cm^{-2}, as shown in Fig. 5c. Compared with the transfer curves obtained under dark conditions, obvious shifts in the transfer curves toward the positive voltage were observed when illuminated with 365-nm light because of the injection of the photo-generated holes into the PEDOT:PSS channel. Meanwhile, as the incident light intensity increased, the output current and photocurrent were significantly enhanced (Fig. S8), which indicated that the OPTs had recovered and maintained their photodetection function after healing.

To further evaluate the photosensitivity performance of self-healing OPTs, responsivity (R), and detectivity (D*), which are two important figures of merit, can be calculated using the following equations [38]:

$$R = \frac{I_{\text{light}} - I_{\text{dark}}}{P \cdot S} = \frac{I_{\text{ph}}}{P \cdot S}, \quad (1)$$

$$D^* = \frac{\sqrt{S \cdot \Delta f}}{\text{NEP}}, \quad (2)$$

$$\text{NEP} = \frac{\sqrt{i_n^2}}{R}, \quad (3)$$

where I_{light} and I_{dark} are the current under light illumination and dark conditions, respectively, P is the optical power intensity, S is the effective working area of the devices, Δf is the bandwidth of the device, NEP is the noise equivalent power, and $(i_n^2)^{1/2}$ is the root-mean-square value of the noise current. Fig. S9 shows the actual noise current of 10^9 A Hz$^{1/2}$ acquired from a lock-in amplifier to accurately evaluate the value of D*. Fig. 5d shows the gate-voltage-dependent R, and the values of R and D* decrease with the increase in the light intensity because of the enhanced photocarrier recombination at higher light power intensity, as shown in Fig. 5e. The resulting R and D* as high as 1.01 × 10^5 A W^{-1} and 1.75 × 10^{12} Jones, respectively, corresponding to an EQE of 3.03 × 10^4% (Fig. S10), were achieved when the light power intensity was as low as 5 μW cm^{-2}. A detailed comparison of the key performance parameters of the reported UV light OPTs is summarized in Table S1, in which the performance of OPTs based on OECT considerably exceeds most of the reported FET-based OPTs for UV detection under low operating voltage [7,8,39–43]. The time-dependent photoresponse behavior of the self-healing OPTs was further investigated by periodically turning the light illumination on and off, as shown in Fig. 5f. The devices exhibited highly stable and reproducible characteristics under light switching and modulation and relatively fast photoresponse speed, in which the rise and fall times were determined to be 0.10 and 0.24 s (Fig. 5g), respectively. Fig. 5h shows the corresponding energy level diagrams of CdSe/ZnS QDs, PEDOT:PSS, and Au obtained using UV–vis and UPS (Figs S11 and S12) and from the literature [44]. The type II band alignment between CdSe/ZnS QDs and PEDOT:PSS favorably enables the photo-generated charge to separate because the large band offsets can induce a strong built-in field [44]. A mass of the photo-generated excitons was generated in the CdSe/ZnS QDs when illuminated by the 365-nm incident light. Consequently, these excitons were rapidly dissociated at the heterojunction interface, and the photo-generated holes were transferred to the PEDOT:PSS channel *via* the potential bias and built-in field, whereas the photo-generated electrons were left behind in the CdSe/ZnS QDs, thereby forming photocurrent and enhanced output current, as shown in Fig. 5i.

Based on the self-healing OPTs photosensing mechanism, the

© Science China Press 2024

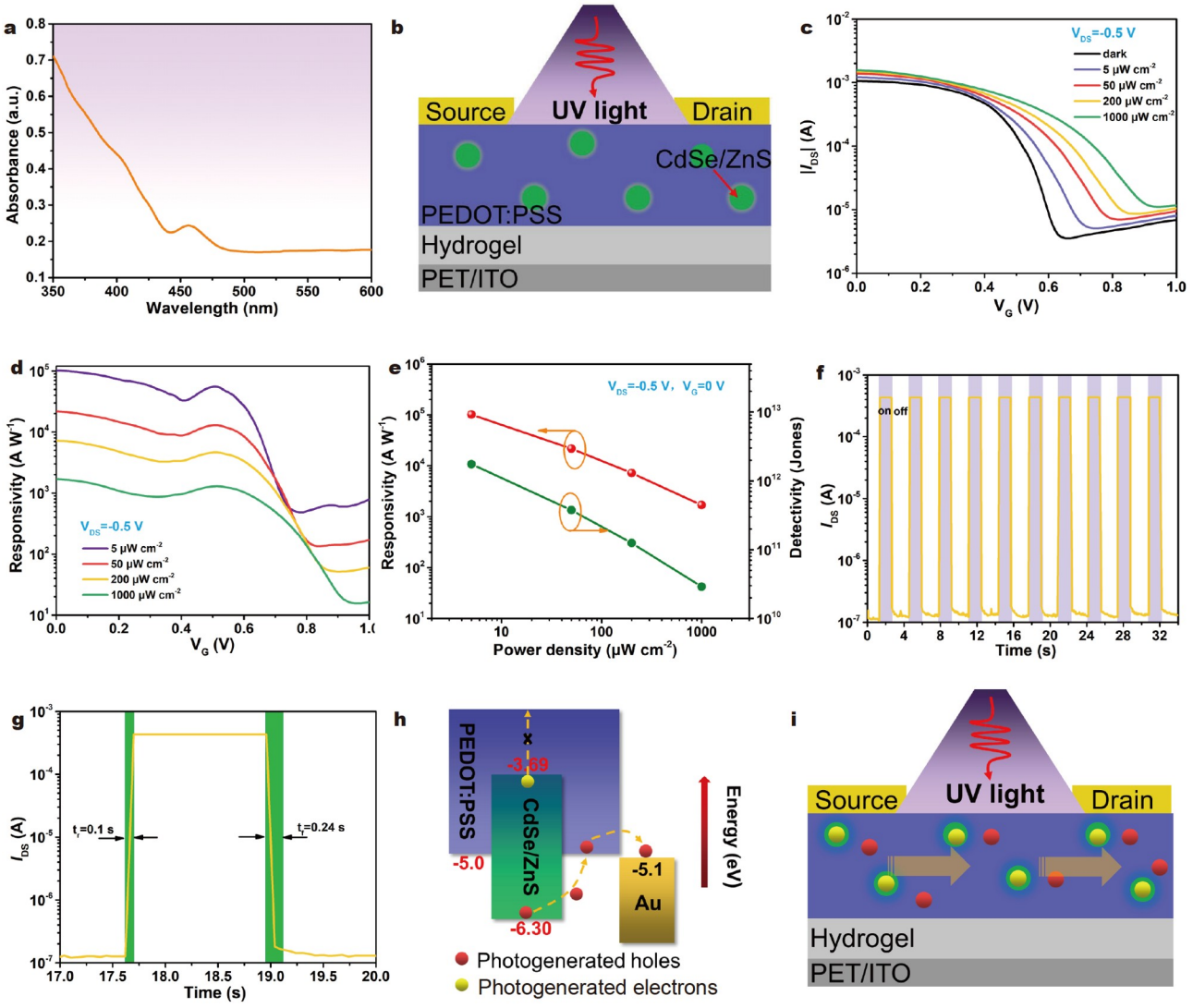

Figure 5 (a) Absorption spectrum of the CdSe/ZnS QDs film. (b) Schematic illustration of the self-healing OPT working under UV light illumination. (c) Transfer characteristic curves under dark and UV light (365 nm) illumination conditions with different incident UV light intensities. (d) Responsivity as a function of the gate voltage at different UV light intensities. (e) Responsivity and detectivity of the device as a function of incident UV light intensity. (f) Time-dependent photoresponse of the device under UV light illumination. The power intensity is 1000 μW cm^{-2}. (g) A single modulation cycle. The rise and fall times are 0.1 and 0.24 s, respectively. (h, i) Energy level and UV-light-induced photocurrent mechanism diagrams of the self-healing OPT.

reasons for the high optoelectronic performance in terms of responsivity, detectivity, and EQE are explained. First, because of their high transconductance value, the incident light served as an additional gate that can regulate the charge density in the PEDOT:PSS channel and amplify the light signal into the detected output current, thus enhancing the photocurrent [21]. More importantly, because of their volumetric charge transport property, the dissociated photo-generated holes could be directly transported to the drain electrode without transferring to the semiconductor/dielectric interface, as shown in Fig. S13, resulting in the increased density of the photo-generated holes in the PEDOT:PSS channel and the enhanced output current. Therefore, the high optoelectronic performance of the self-healing OPTs is attributed to the high transconductance and volumetric charge transport, which amplify the light signal into the electronic current and simultaneously increase the density of the photo-generated holes in the channel significantly, thereby enhancing the photocurrent and ultimately improving the responsivity, detectivity, and EQE.

Healing mechanism of the phototransistors based on composite films

Finally, the healing mechanism of the self-healing OPTs using CdSe/ZnS-PEDOT:PSS/hydrogel composite films was investigated. The healing capability of the CdSe/ZnS-PEDOT:PSS channel is mainly determined by the PEDOT:PSS component. The PEDOT:PSS film comprises a large number of PEDOT:PSS grains that contain conductive PEDOT-rich cores and insulating PSS-rich shells, as shown in Fig. 6b (top), in which the PEDOT:PSS grains are connected through the dynamic hydrogen bonds on the sulfonate groups (R-SO_3^-) of the PSS shells and the electrostatic force between PEDOT and PSS chains [45,46]. Water uptake, which induced the swelling of the PSS chains resulted from the hydrophilic feature, plays a critical role in healing the PEDOT:PSS film [47]. Once the PEDOT:PSS film was mechanically damaged, its water uptake capability enabled

 © Science China Press 2024

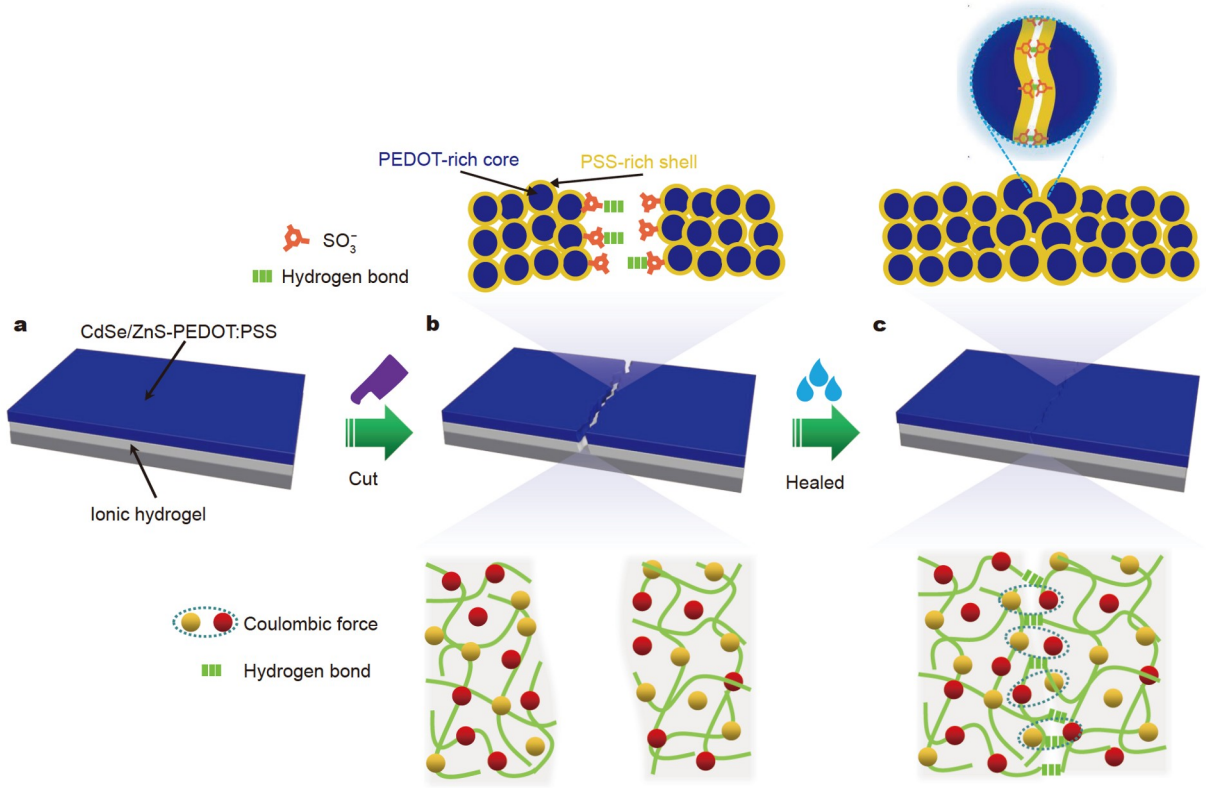

Figure 6 (a) Schematic illustration of the fresh CdSe/ZnS-PEDO:PSS/hydrogel composite film before cutting. (b, c) Schematic of the healing mechanisms of CdSe/ZnS-PEDO:PSS (top) and ionic hydrogel film (bottom).

the rapid volumetric swelling and spreading of the PSS chains toward the damaged site after uptaking water. Meanwhile, the spreading of the PSS chains enabled the diffusion of the PEDOT chains into the damaged area because PEDOT and PSS chains are entangled with each other [48], followed by the reformation of the dynamic hydrogen bonds, electrostatic force, and PEDOT$^+$-PEDOT$^+$ conducting path across the damaged area, as shown in Fig. 6c (top). Thus, the PEDOT:PSS film with incision was efficiently healed and restored its electrical performance. For the ionic hydrogel film, the chitosan chains were interconnected by the hydrogen bonds benefiting from the abundant carboxyl and hydroxyl groups on the chitosan backbones [49]. The DI water not only provided additional hydrogen bonds as a bridge across the damaged area but also increased the mobile chitosan chains. Ultimately, the reformation of the hydrogen bonds and coulombic force between Li^+ and $[TFSI]^-$ ions contributed to healing of the damaged ionic hydrogel film, as shown in Fig. 6c (bottom) [50,51].

CONCLUSIONS

In summary, intrinsically healable, high-performance, and flexible phototransistors with strong healing capability were developed using the healing PEDOT:PSS channel and ionic hydrogel electrolyte. The self-healing OPTs can restore their mechanical and electronic performance and maintain high optoelectronic functionality upon severe damage from blade cutting. The volumetric swelling feature of PSS^- chains mainly contributes to the healing of the CdSe/ZnS-PEDOT:PSS channel through the reformation of the dynamic hydrogen bonds, electrostatic force, and PEDOT$^+$-PEDOT$^+$ conducting path across the damaged area. Meanwhile, the dynamic hydrogel bonds and coulombic force between Li^+ and $[TFSI]^-$ ions can be reformed to repair the damaged ionic hydrogel film and thus restore its mechanical and electronic properties. Moreover, the CdSe/ZnS-PEDOT:PSS/hydrogel composite films can be dissolved in water, exhibiting their biodegradability. Furthermore, the self-healing OPTs exhibit excellent responsivity as high as 1.01×10^5 A W^{-1}, specific detectivity of 1.75×10^{12} Jones, and high EQE of up to 3.03×10^4% at an operating voltage of only 0.5 V, which considerably exceed the values of most the reported OPTs using the FET architecture for UV detection. The high optoelectronic performance of the self-healing OPTs is attributed to the high transconductance and volumetric charge transport, which amplify the light signal into the electronic current and simultaneously increase the density of the photo-generated holes in the channel significantly, thereby enhancing the photocurrent. Our findings provide a facile, low-cost, and effective device system to develop an intrinsically healing, degradable, and high-performance phototransistor for next-generation optoelectronic devices.

Received 10 November 2023; accepted 26 January 2024; published online 1 April 2024

1 An C, Nie F, Zhang R, *et al.* Two-dimensional material-enhanced flexible and self-healable photodetector for large-area photodetection. Adv Funct Mater, 2021, 31: 2100136
2 Lee YH, Park S, Won Y, *et al.* Flexible high-performance graphene hybrid photodetectors functionalized with gold nanostars and perovskites. NPG Asia Mater, 2020, 12: 79
3 Zhang Y, Qiu Y, Li X, *et al.* Organic single-crystalline microwire arrays toward high-performance flexible near-infrared phototransistors. Small, 2022, 18: e2203429

 © Science China Press 2024

4 Chow PCY, Someya T. Organic photodetectors for next-generation wearable electronics. Adv Mater, 2020, 32: 1902045
5 Ahn S, Chen W, Moreno-Gonzalez MA, *et al.* Enhanced charge transfer and responsivity in hybrid quantum dot/graphene photodetectors using ZnO as intermediate electron-collecting layer. Adv Elect Mater, 2020, 6: 2000014
6 Chang YH, Ku CW, Zhang YH, *et al.* Ultrafast responsive non-volatile flash photomemory *via* spatially addressable perovskite/block copolymer composite film. Adv Funct Mater, 2020, 30: 2000764
7 Guo J, Jiang S, Pei M, *et al.* Few-layer organic crystalline van der Waals heterojunctions for ultrafast UV phototransistors. Adv Elect Mater, 2020, 6: 2000062
8 Zou C, Xi Y, Huang C, *et al.* A highly sensitive UV-vis-NIR all-inorganic perovskite quantum dot phototransistor based on a layered heterojunction. Adv Opt Mater, 2018, 6: 1800324
9 Simone G, Dyson MJ, Meskers SCJ, *et al.* Organic photodetectors and their application in large area and flexible image sensors: The role of dark current. Adv Funct Mater, 2020, 30: 1904205
10 Zhao Z, Xu C, Niu L, *et al.* Recent progress on broadband organic photodetectors and their applications. Laser & Photonics Rev, 2020, 14: 2000262
11 Calvi S, Rapisarda M, Valletta A, *et al.* Highly sensitive organic phototransistor for flexible optical detector arrays. Org Electron, 2022, 102: 106452
12 Huang X, Liu Y, Liu G, *et al.* Short-wave infrared synaptic phototransistor with ambient light adaptability for flexible artificial night visual system. Adv Funct Mater, 2023, 33: 2208836
13 Kim JH, Stolte M, Würthner F. Wavelength and polarization sensitive synaptic phototransistor based on organic n-type semiconductor/supramolecular J-aggregate heterostructure. ACS Nano, 2022, 16: 19523–19532
14 Wang M, Sun H, Cao F, *et al.* Moisture-triggered self-healing flexible perovskite photodetectors with excellent mechanical stability. Adv Mater, 2021, 33: 2100625
15 Cai S, Xu X, Yang W, *et al.* Materials and designs for wearable photodetectors. Adv Mater, 2019, 31: 1808138
16 Gu P, Yao Y, Feng L, *et al.* Recent advances in polymer phototransistors. Polym Chem, 2015, 6: 7933–7944
17 Huang X, Ji D, Fuchs H, *et al.* Recent progress in organic phototransistors: semiconductor materials, device structures and optoelectronic applications. ChemPhotoChem, 2019, 4: 9–38
18 Yan Y, Yu R, Gao C, *et al.* High-performance n-type thin-film transistor based on bilayer MXene/semiconductor with enhanced electrons transport. Sci China Mater, 2022, 65: 3087–3095
19 Di C, Liu Y, Yu G, *et al.* Interface engineering: An effective approach toward high-performance organic field-effect transistors. Acc Chem Res, 2009, 42: 1573–1583
20 Rivnay J, Inal S, Salleo A, *et al.* Organic electrochemical transistors. Nat Rev Mater, 2018, 3: 17086
21 Sun H, Gerasimov J, Berggren M, *et al.* n-Type organic electrochemical transistors: Materials and challenges. J Mater Chem C, 2018, 6: 11778–11784
22 Friedlein JT, McLeod RR, Rivnay J. Device physics of organic electrochemical transistors. Org Electron, 2018, 63: 398–414
23 Massetti M, Zhang S, Harikesh PC, *et al.* Fully 3D-printed organic electrochemical transistors. Npj Flex Electron, 2023, 7: 11
24 Koutsouras DA, Torricelli F, Blom PWM. Submicron vertical channel organic electrochemical transistors with ultrahigh transconductance. Adv Elect Mater, 2023, 9: 2200868
25 Rivnay J, Leleux P, Sessolo M, *et al.* Organic electrochemical transistors with maximum transconductance at zero gate bias. Adv Mater, 2013, 25: 7010–7014
26 Tan STM, Giovannitti A, Melianas A, *et al.* High-gain chemically gated organic electrochemical transistor. Adv Funct Mater, 2021, 31: 2010868
27 Montero-Jimenez M, Amante FL, Fenoy GE, *et al.* PEDOT-polyamine-based organic electrochemical transistors for monitoring protein binding. Biosensors, 2023, 13: 288
28 Huang W, Chen J, Yao Y, *et al.* Vertical organic electrochemical transistors for complementary circuits. Nature, 2023, 613: 496–502
29 Fu Y, Wang N, Yang A, *et al.* Highly sensitive detection of protein biomarkers with organic electrochemical transistors. Adv Mater, 2017, 29: 1703787
30 Venkatraman V, Friedlein JT, Giovannitti A, *et al.* Subthreshold operation of organic electrochemical transistors for biosignal amplification. Adv Sci, 2018, 5: 1800453
31 Wang C, Wu H, Chen Z, *et al.* Self-healing chemistry enables the stable operation of silicon microparticle anodes for high-energy lithium-ion batteries. Nat Chem, 2013, 5: 1042–1048
32 Chortos A, Liu J, Bao Z. Pursuing prosthetic electronic skin. Nat Mater, 2016, 15: 937–950
33 Guan Q, Lin G, Gong Y, *et al.* Highly efficient self-healable and dual responsive hydrogel-based deformable triboelectric nanogenerators for wearable electronics. J Mater Chem A, 2019, 7: 13948–13955
34 Kee S, Haque MA, Corzo D, *et al.* Self-healing and stretchable 3D-printed organic thermoelectrics. Adv Funct Mater, 2019, 29: 1905426
35 Ko J, Surendran A, Febriansyah B, *et al.* Self-healable electrochromic ion gels for low power and robust displays. Org Electron, 2019, 71: 199–205
36 Kwon S, Kim J, Kim G, *et al.* Organic single-crystal semiconductor films on a millimeter domain scale. Adv Mater, 2015, 27: 6870–6877
37 Lv Z, Zhou Y, Han ST, *et al.* From biomaterial-based data storage to bio-inspired artificial synapse. Mater Today, 2018, 21: 537–552
38 Baeg KJ, Binda M, Natali D, *et al.* Organic light detectors: Photodiodes and phototransistors. Adv Mater, 2013, 25: 4267–4295
39 Bai S, Yang L, Haase K, *et al.* Nanographene-based heterojunctions for high-performance organic phototransistor memory devices. Adv Sci, 2023, 10: 2300057
40 Shin H, Kim D, Park J, *et al.* Improving photosensitivity and transparency in organic phototransistor with blending insulating polymers. Micromachines, 2023, 14: 620
41 Qiu LZ, Wei SY, Xu HS, *et al.* Ultrathin polymer nanofibrils for solar-blind deep ultraviolet light photodetectors application. Nano Lett, 2020, 20: 644–651
42 Li B, Zhang Y, Liu Y, *et al.* Highly efficient contact doping for high-performance organic UV-sensitive phototransistors. Crystals, 2022, 12: 651
43 Lou Y, Shi R, Yu L, *et al.* A new dithieno[3,2-*b*:2′,3′-*d*]thiophene derivative for high performance single crystal organic field-effect transistors and UV-sensitive phototransistors. RSC Adv, 2023, 13: 11706–11711
44 Li D, Jia Z, Tang Y, *et al.* Inorganic–organic hybrid phototransistor array with enhanced photogating effect for dynamic near-infrared light sensing and image preprocessing. Nano Lett, 2022, 22: 5434–5442
45 Romele P, Ghittorelli M, Kovács-Vajna ZM, *et al.* Ion buffering and interface charge enable high performance electronics with organic electrochemical transistors. Nat Commun, 2019, 10: 3044
46 Rivnay J, Inal S, Collins BA, *et al.* Structural control of mixed ionic and electronic transport in conducting polymers. Nat Commun, 2016, 7: 11287
47 Groenendaal L, Jonas F, Freitag D, *et al.* Poly(3,4-ethylenedioxythiophene) and its derivatives: Past, present, and future. Adv Mater, 2000, 12: 481–494
48 Dupont SR, Novoa F, Voroshazi E, *et al.* Decohesion kinetics of PEDOT:PSS conducting polymer films. Adv Funct Mater, 2014, 24: 1325–1332
49 Xu C, Nie J, Wu W, *et al.* Design of self-healable supramolecular hybrid network based on carboxylated styrene butadiene rubber and nanochitosan. Carbohydrate Polyms, 2019, 205: 410–419
50 Cao Y, Tan YJ, Li S, *et al.* Self-healing electronic skins for aquatic environments. Nat Electron, 2019, 2: 75–82
51 Xia S, Song S, Jia F, *et al.* A flexible, adhesive and self-healable hydrogel-based wearable strain sensor for human motion and physiological signal monitoring. J Mater Chem B, 2019, 7: 4638–4648

Acknowledgements The work was supported by the National Natural Science Foundation of China (62304189 and 62304002), the Natural Science Foundation of Xiamen City (3502Z20227063), the Natural Science Founda-

 © Science China Press 2024

tion of Fujian Province (2023J011450 and 2023J011452), the Key Technologies Innovation and Industrialization Projects of Fujian Province (2023XQ022), the National Natural Science Foundation of China Joint Fund for Cross-strait Scientific and Technological Cooperation (U2005212), and the Open Fund of Xiamen Key Laboratory of High Performance Metal and Materials of Xiamen University.

Author contributions Chen H and Xie A conceived the project. Yan Y, Zhu X, Zhang G, and Wang X designed and performed the experiments and collected the data. Yan Y, Zhu X, Li W, Sun D, Li Y, and Han X analyzed and discusssed the data. Yan Y, Zhu X, Chen H, and Xie A wrote and reviewed the paper. All authors contributed to the general discussion.. All authors have read and agreed to the published version of the manuscript.

Conflict of interest The authors declare that they have no conflict of interest.

Supplementary information Supporting data are available in the online version of the paper.

Yujie Yan is now an associate professor at the School of Materials Science and Engineering, Xiamen University of Technology. He received his PhD degree from Fuzhou University in 2021. His research interest focuses on nanoscale optoelectronic devices including transistors, photodetectors, and electrochromic devices.

An Xie is a full professor at the Department of Materials Science and Engineering, Xiamen University of Technology. He received his PhD degree from the Department of Rock and Mineral Material Science, China University Of Geosciences, Wuhan, in 2010. He worked as a deputy chief engineer and postdoctor at Fushun Optoelectronics Technology Limited Company. His research is focusing on the optoelectronic films and display materials.

Huipeng Chen got his PhD degree from Tufts University in 2009. Before joining the College of Physics and Information Engineering, Fuzhou University in 2015, he worked as a postdoctoral fellow at Texas Tech University during 2009–2011 and the University of Tennessee and Oak Ridge National Laboratory from 2011 to 2014. His research interest is the research of semiconductor materials and devices, including thin film transistors, memories, sensors, and neuromorphic electronic devices and systems.

本征可修复的导电聚合物/水凝胶纳米复合薄膜及其独特的体沟道用于实现高性能、柔性和可修复的有机光电晶体管

严育杰[1,2†*], 朱晓婷[3†], 张国成[4], 汪秀梅[5], 韩笑[1], 李伟洲[1], 孙东亚[1], 李月婵[1], 王义[1], 谢安[1*], 陈惠鹏[2*]

摘要 柔性有机光电晶体管(OPTs)在大机械形变的下一代可穿戴系统中至关重要. 然而, 目前报道的大多数OPTs都是场效应基结构, 其界面电荷传输和本征低跨导的特性限制了OPTs的机械柔性和光电性能的发展. 此外, 沟道层的p共轭半导体聚合物也缺乏特殊的可修复位点, 使其很难实现薄膜的自我修复功能. 本文报道了一个具有独特体沟道和强修复功能的柔性高光电性能的OPTs. 该OPTs使用有机电化学晶体管架构, 由3D体沟道的可修复导电聚合物/水凝胶复合薄膜组成. 该器件不仅在遭受损伤后能够在100 ms内有效恢复其机械和电学性能, 同时还展现出出色的机械柔性. 更重要的是, 该器件实现了紫外光波段的高光测性能, 其中光响应度高达1.01×10^5 A W^{-1}, 探测率达1.01×10^5 A W^{-1}, 外量子效率达3.03×10^4%. 结果表明, 具有独特体沟道和本征可修复功能的OPTs在下一代可穿戴电子器件的使用中具有潜在应用价值.

© Science China Press 2024